

## Interband optical investigation of Bloch oscillations in semiconductor superlattices

This article has been downloaded from IOPscience. Please scroll down to see the full text article.

1998 Semicond. Sci. Technol. 13 249

(<http://iopscience.iop.org/0268-1242/13/3/003>)

View [the table of contents for this issue](#), or go to the [journal homepage](#) for more

Download details:

IP Address: 128.193.96.7

The article was downloaded on 30/04/2012 at 20:25

Please note that [terms and conditions apply](#).

## TOPICAL REVIEW

# Interband optical investigation of Bloch oscillations in semiconductor superlattices

Karl Leo

Institut für Angewandte Photophysik, Technische Universität Dresden,  
D-01062 Dresden, Germany

Received 11 August 1997, accepted for publication 22 October 1997

**Abstract.** The experimental observation of Bloch oscillations in solids was long thought to be out of experimental reach. The invention of the semiconductor superlattice has changed this situation decisively. Transport experiments performed in the past two decades have given indirect evidence for the existence of Bloch oscillations. Recently, it has been possible to directly observe Bloch oscillations in semiconductor superlattices by optical experiments: interband laser excitation of several Wannier–Stark ladder states creates a wave packet which oscillates in time with a characteristic dependence on the static electric field. These oscillations have been observed by several optical methods, both using detection of the interband polarization (four-wave mixing and photorefractive sampling) and intraband polarization (THz emission spectroscopy). The latter experimental technique directly proves the emission of radiation at the Bloch oscillator frequency. Recent experiments have directly measured the displacement of the Bloch wave packet as a function of time, proving the harmonic dependence as predicted by Zener. A number of experiments have addressed other key physical parameters of Bloch oscillations like the damping mechanisms. This article gives a brief review of recent investigations of Bloch oscillations in superlattices, focused on the interband optical experiments performed in the last few years.

## 1. Introduction

### 1.1. Bloch oscillations and the Wannier–Stark ladder

The standard picture of electronic transport in solids when a static field is applied is drift transport as first considered in detail by Drude [1]: carriers move ballistically until they change their momentum by a scattering process. The drift velocity of the carriers is determined by a balance between the momentum and energy gain from the field during ballistic motion and by the momentum and energy changes due to elastic and inelastic scattering processes. The overall current due to the moving carriers is then characterized by Ohm's law

$$\mathbf{j} = \sigma \mathbf{E}. \quad (1.1)$$

The conductivity  $\sigma$  is in the Drude picture given by

$$\sigma = \frac{e^2 n \tau}{m} \quad (1.2)$$

where  $\tau$  is the momentum relaxation time,  $n$  the carrier density and  $m$  the carrier mass.

One of the central assumptions of the Drude picture is that the carrier move ballistically between scattering events.

A description as free carriers is well justified if the carriers stay close to the lower band edge. However, if the fields are high enough that the carriers reach higher parts of the bands before they are scattered, the electrons do not behave like free carriers anymore: if the scattering rate is low enough, they start to oscillate. This fact follows directly from the properties of the electronic band structure of a crystalline solid under the influence of a static electric field: Bloch has shown [2] in 1928 that an electron in a periodic potential subject to an external electric field  $F$  changes its  $k$ -vector according to

$$h \frac{dk}{dt} = eF. \quad (1.3)$$

Since the band structure is periodic in  $k$ , it is immediately obvious (as pointed out by Zener [3]) that an electron which is not subject to scattering processes will perform an oscillatory motion in energy (see figure 1). This oscillatory motion in energy is accompanied by a periodic motion in real space, the so-called Bloch oscillations (BOs). The time period of the motion is given by

$$\tau_B = \frac{h}{eFd} \quad (1.4)$$

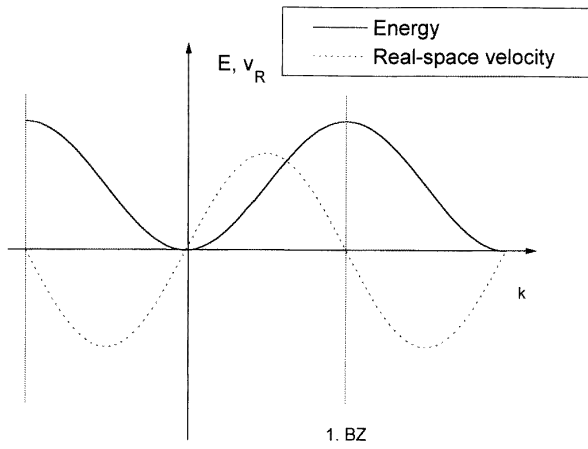


**Figure 1.** Bloch oscillations in the semi-classical picture. An electron at  $k = 0$  starts to move with constant velocity in  $k$ -space once the field is turned on. Until the edge of the first Brillouin zone, it gains energy. When it leaves the first Brillouin zone, the energy starts to decrease and the velocity (dashed line) becomes negative. When it reaches the centre of the second Brillouin zone, it has returned to its original spatial position.

(with  $d$  as the period of the lattice) and the total spatial extension (from left to right maximum of the oscillation displacement) by

$$L = \frac{W}{eF} \quad (1.5)$$

where  $W$  is the width of the band. Figure 1 (after [4]) shows a scheme of the first Brillouin zone of a crystalline solid with the energy of the electron  $E$  (solid line) and its real space velocity  $v_R$  (dashed line) given by

$$v_R = \frac{\partial E}{\partial k}. \quad (1.6)$$

In the first half of its cycle, the electron moves with the field and gains energy from the field; in the second half, it moves against the field and loses energy to it [5]. The periodic motion can also be understood as a Bragg reflection of the accelerated electron once its wavelength reaches the lattice period. It is interesting to note that the phenomenon of Bloch oscillations is rather independent of the details of the band structure: the equations given for amplitude and period are generally valid.

The criterion which divides Drude drift transport from Bloch oscillations is the ratio of the scattering time  $\tau$  to the BO period  $\tau_B$ : only if  $\tau$  is large compared to  $\tau_B$  will the oscillations occur. The observation of BOs thus requires high fields and/or long scattering times.

The effect of a static field on a periodic band structure can as well be discussed in a real space picture: the eigenstates of the lattice without field are the well known Bloch functions which are infinitely extended. Once a field is applied, the wave functions become localized with a localization length  $L$  which is identical to that given in (1.5). The energy spectrum of the lattice subject to an electric field is no longer a continuous band, but consists [6] of the so-called Wannier–Stark ladder (WSL) with energies

$$E = E_0 + n\Delta E \quad (1.7)$$

where  $\Delta E$  is the ladder spacing given by

$$\Delta E = eFd \quad (1.8)$$

$n$  is a natural number and  $E_0$  is the energy of a particular reference state.

Similarly to their time domain counterpart, the observation of the Wannier–Stark ladder requires certain conditions. The wave functions at zero field are in a real system not completely delocalized, but have a certain coherence length which depends on the scattering processes the electronic states are subject to. The Wannier–Stark localization can only occur if the field localization length  $L$  is smaller than the scattering localization length. It is obvious that this criterion is equivalent to the condition that the scattering time is longer than the BO period.

## 1.2. Experimental observation of Bloch oscillations

For many years, it has been controversially debated whether Bloch oscillations and the Wannier–Stark ladder exist. In the centre of a theoretical debate about the existence of the Wannier–Stark ladder was the question whether field localization and the observation of the ladder would be prevented by coupling to higher bands and the continuum: the ladder states are not stationary, since scattering to higher bands and the continuum can take place. The debate whether coupling to higher states prevents the existence of the WSL has seemingly been settled with the result that the coupling to other states is under certain conditions weak enough to preserve the ladder structure. The experimental observations of the WSL and BO as discussed in this review have naturally confirmed this result.

Similarly, the experimental observability of BOs has been debated for many years. The main obstacle to the observation of BOs in bulk solids is that the electron has to gain a large amount of energy (a few eV in most solids) to be reflected. At such high energies, the relaxation by scattering processes is very fast, making the completion of a full oscillation period unlikely. If the electron is scattered long before it reaches the edge of the Brillouin zone, it stays at small  $k$ -vectors and moves always into the field direction, i.e. it is subject to standard drift transport.

A dramatic improvement for the observation of BO came with the invention of the semiconductor superlattice by Esaki and Tsu in the early 1970s [7]. By the alternating growth of semiconductor layers with larger and smaller band gap, a superlattice is created in the growth ( $z$ -) direction (see figure 2, upper part). If the barrier layers are sufficiently thin, the coupling between the electronic states in the wells leads to the formation of a so-called miniband in the  $z$ -direction. Typical band widths are of the order of 20–200 meV. The much smaller band widths compared to bulk semiconductors allow to perform experiments at much lower fields. Related is the fact that the electrons need to reach much lower energies than in conventional solids to get to the upper part of the band, thus reducing the scattering probability with, e.g. optical phonons. The experimental realization of semiconductor superlattices (starting with [8]) enabled immediately a number of experiments which demonstrated the influence of the novel electronic states

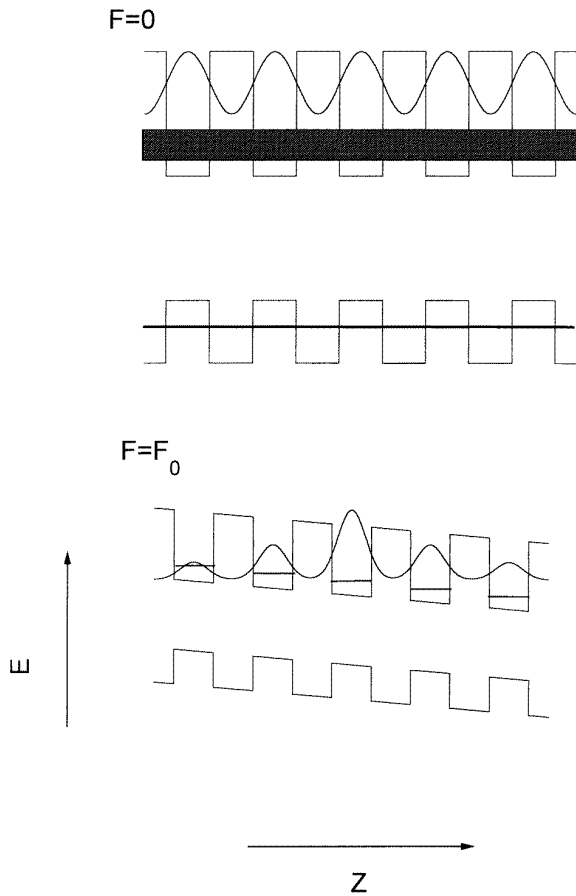


**Figure 2.** Schematic picture of a type I semiconductor superlattice without applied field (upper part) and with applied field (lower part). The probability amplitudes of the electronic states are also sketched.

on transport or optical properties [9–11]. However, in all of the transport experiments, the observed experimental parameters were determined for the ensemble average, and the oscillation of individual electrons was averaged out. For a direct observation of the oscillations, it is necessary to create a carrier ensemble with defined phase relations.

The recent advances in ultrafast laser technology have made it possible to create electronic excitations in atoms, molecules and solids with well defined phase. By excitation with short laser pulses, wave packet states with defined relative phase can be created. First experiments which showed wave packet dynamics were using superpositions of electronic states without particular spatial dynamics, like quantum beats between light-hole and heavy-hole excitons in quantum wells.

The first experiments which demonstrated *spatial* dynamics of wave packets in solids were observing coherent oscillations of electrons in double quantum wells [12]. In these experiments, a localized wave function is created in one of the wells by a superposition of the symmetric and antisymmetric wave function. This wave packet oscillates between the wells with a frequency given by the energy difference between the two states. It was shown by Roskos *et al* [13] that the oscillation of the wave packet leads to emission of THz radiation.

Recently, Bloch oscillations *were directly observed by optical techniques*. In these experiments, a localized wave packet is created in a biased semiconductor superlattice. This wave packet performs spatial oscillations with the period given by (1.4). For the detection of the Bloch wave packet motion, a number of experimental techniques have been used: the first experiments used four-wave mixing (FWM) [14, 15]; later THz emission spectroscopy [16], photorefractive experiments [17] and time-resolved transmission spectroscopy [18] were employed. The purpose of this article is to review the recent studies, relate them to transport experiments and discuss possible further experiments.

The outline of the article is as follows. After this introduction, a brief overview of the properties of superlattices (SLs) is given (section 1.3). Then, the optical experiments leading to the direct observation of BOs are discussed (section 2). After a few general remarks, including a discussion of the often-asked question of how the optical experiments are related to transport observations of BOs, the subsequent sections describe in detail the first four-wave mixing experiments (section 2.2). Later, more detailed four-wave mixing experiments investigating the quantum nature of the oscillations and the miniband dependence (section 2.3) are discussed, followed by THz emission experiments (section 2.4). The section is concluded with two sections discussing recent investigations of the spatial displacement of the wave packet (2.5) and the damping mechanisms of BOs (2.6)

In the second part of the article (section 3), a comparison to transport experiments (section 3.1) is made and possible further experiments (section 3.3 which addresses open questions about the physics of Bloch oscillations) are discussed. The article concludes with some aspects of the realization of devices.

### 1.3. Semiconductor superlattices

The proposal of the *semiconductor superlattice* by Esaki and Tsu [7] was a key step towards the observation of Bloch oscillations. By the alternating growth of thin semiconductor layers with smaller and larger bandgap, it is possible to design new forms of one-dimensional crystals with properties which are much more benign for BOs: by suitable adjustment of the period and the band gap difference, the band width of the artificially created band in the growth direction (the so-called miniband) can in principle be adjusted between zero and a few hundred meV. Figure 2 (upper part) scheme shows a schematic picture of a semiconductor superlattice with the electron and hole minibands. Note that we display here the special case of a type I superlattice, where the bands of the material with smaller band gap are located (in energy) between the bands of the material with larger band gap.

The electronic states in semiconductor superlattices and other heterostructures are usually calculated using the envelope approach [19] where it is assumed that the Bloch functions stay unchanged in the respective materials and that only the oscillating part of the wave function is

changed. The problem reduces in the simplest case (one-band approximation) to a solution of a one-dimensional Schrödinger equation for the envelope function

$$\left( \frac{-\hbar^2}{2m^*} \nabla^2 + V_{C,V} \Psi(r) \right) = E \Psi(r) \quad (1.9)$$

where  $V_{C,V}$  is the periodic superlattice potential. The dispersion relation of the superlattice miniband can be expressed in a transcendental equation which can only be solved numerically. For many cases, the nearest-neighbour approximation can be made and the dispersion relation in the  $z$ -direction for the lowest miniband reads then

$$E(k) = \frac{W_1 + W_2}{2} + W \cos kd \quad (1.10)$$

where  $W_1$  and  $W_2$  are the lower and upper edge of the miniband and  $W = W_2 - W_1$  is the miniband width. For higher minibands, the dispersion relation is inverted. Additionally to the miniband dispersion, the dispersion in the  $x$ - and  $y$ -directions has to be included. The full dispersion is then the sum of the  $z$ -dispersion (1.10) and the usual parabolic dispersions in the  $x$ - and  $y$ -directions.

The width of the minibands in semiconductor superlattices can be controlled over a large energy range by choosing appropriate materials systems and layer thickness. The large majority of experiments in SLs have used the GaAs/Al<sub>x</sub>Ga<sub>1-x</sub>As heterosystem due to the superior quality of the samples. If the material is kept direct in the barrier (i.e. the aluminium content of the barriers is kept below about  $x = 0.4$ ), the available total band offset is about 0.5 eV. Assuming a 2/3 to 1/3 ratio of the band offsets for the conduction and the valence band, the maximum offset of the conduction band and thus the maximum width of the electron miniband is about 300 meV in this system. The lower limit for miniband widths depends on scattering processes and also on sample quality: it only makes sense to talk about a miniband if the broadening due to both sample imperfections and scattering is lower than the miniband width. In practice, these factors will limit the miniband width to values above a few meV at low temperature. In optical experiments, the miniband coupling can be prevented by the Coulomb interaction [20]. It can be shown that the lower limit for the miniband width is approximately given by the exciton binding energy, which is between 5 and 10 meV in the III–V systems.

## 2. Optical experiments observing Bloch oscillations in superlattices

### 2.1. General remarks

How is it possible to observe Bloch oscillations? Most simple, but still a Gedanken experiment in solids, is the original approach to ‘put’ one electron at  $k = 0$ , ‘turn on’ the field at  $t = 0$  within a time span much shorter than  $\tau_B$ , and observe the oscillating current with sufficient time resolution. This experiment has not been performed in solids yet, in particular due to the extremely fast switching of the field which is required and the problem

of measuring the current with sufficient time resolution. It is interesting to note that it was recently possible to perform an experiment in an artificial ‘lattice’ (consisting of an optical standing wave) in which atoms were performing Bloch oscillations. This experiment comes very close to the Gedanken experiment just described [21].

More realistic approaches for electrical measurements are experiments where a macroscopic current through a p-n diode is measured. In semiconductor superlattices, these experiments have brought a wealth of new information. In particular, it was shown that negative differential velocity (NDV) occurs at higher fields [22], confirming the prediction of Esaki and Tsu. The observation of NDV is caused by the fact that many of the electrons reach higher parts of the miniband with negative effective mass, i.e. the real-space velocity is decreasing with increasing energy. It can be predicted that such standard transport experiments will not lead to the observation of BOs since the electron ensemble participating in the total current is entering the regions with high field with arbitrary phase. Thus, the oscillatory motion of the individual electrons is averaged out, and the external current flow represents the ensemble motion, which is a slow motion in the field direction due to the inevitable scattering events which take place even if the conditions for BOs of the individual electron are given. Nevertheless, the observation of NDV is already a proof that the upper parts of the band are reached by a fraction of the electrons. It is thus very likely that a few of them will perform complete Bloch cycles, which are masked by the slowly drifting ensemble.

The requirement for defined phase relation of the electrons *can be easily reached with optical experiments*, where carriers with defined phase are created with a coherent light source. Optical experiments with cw excitation in semiconductor superlattices have yielded important information. The most impressive result has been the first observation of the Wannier–Stark ladder (WSL) by Mendez and coworkers [23] and Voisin and coworkers [24]: the experiments showed that the optical response for finite static fields is governed by a ladder of optical transitions with energies

$$E_n = E_0 + neFd \quad n = 0, \pm 1, \pm 2, \dots \quad (2.1)$$

where  $E_0$  corresponds to a transition from electrons and holes located in the same well (see figure 3). These experiments directly prove that the eigenstates of a superlattice subject to an excited field are localized to a few wells and have a ladder-like energy spectrum (as depicted in figure 2, lower part). The optical experiments in SLs have definitely ended the theoretical dispute about the existence of the WSL. Figure 3 shows schematically the states in a biased semiconductor superlattice and the WSL. It is a characteristic feature of III–V superlattices that the heavy holes are strongly localized due to their large mass. Thus, the optical transitions reflect mostly the electron WSL. If the optical transition energies are monitored as a function of the bias field, a characteristic fan chart results (figure 3).

The discovery of the Wannier–Stark ladder in superlattices [23, 24] can be regarded as a proof that Bloch oscillations must exist in those systems. The first discussion

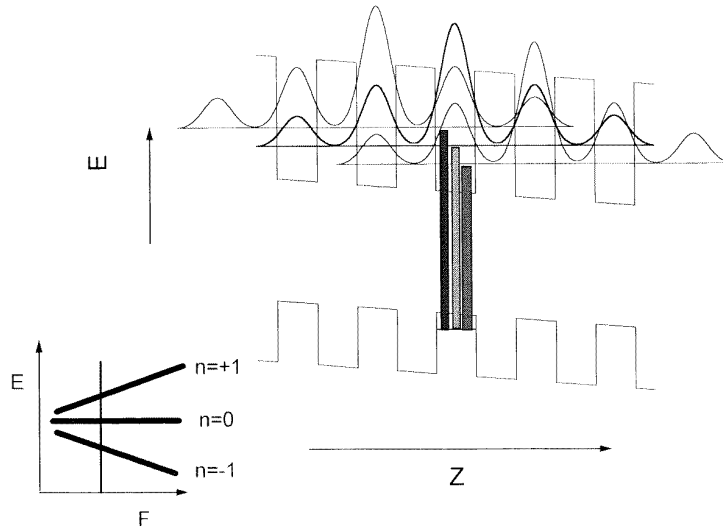


**Figure 3.** Scheme of the optical transitions in a biased semiconductor superlattice characterized by spatially direct and indirect transitions, leading to a fan chart when the field is swept (inset).

which addressed BOs in superlattices in detail was a theoretical paper by Bastard and Ferreira [25], which treated the dynamics of superpositions of WS states. In particular, the authors considered the dynamics of a wave packet with initial conditions chosen such that it was localized in one well. They showed that it oscillates with  $\tau_B$ , similar to the wave packet in the Gedanken experiment described above. However, the spatial motion for the initial conditions chosen (which corresponded approximately to symmetric optical excitation of the centre of the WSL) results in a spatially symmetric *breathing motion* of the wave packet, without an associated oscillating dipole moment.

The next step after the cw observation of the WSL was to perform experiments with short-pulse optical excitation in superlattices. If the spectral pulse width is larger than the spacing between two adjacent levels of the WSL (which is practically equivalent to the requirement that the optical pulse is shorter than the period of a BO), one creates a wave packet from a superposition of Wannier–Stark states. This superposition of WS states will oscillate due to a quantum interference (quantum beats) with a period

$$\frac{h}{\Delta E} = h/eFd = \tau_B \quad (2.2)$$

which is the BO frequency mentioned in (1.4). It should be noted that the pure observation of these quantum beats is a corollary of the observation of the WSL in frequency space. Nevertheless, the observation of the WSL is not a prerequisite of a BO interference in the time domain: for strong inhomogeneous broadening of the system, BO might be observed despite the fact that the WSL is smeared out in the optical spectra.

An obvious question is whether the optical experiments observing quantum beats of the WSL are related to Bloch oscillations. It can be easily argued that they are virtually the same physical phenomenon. The argumentation for this claim is as follows [26]: the electron which is ‘put’ in the Gedanken experiment at  $k = 0$  can be expressed as

a wave packet of Bloch states (which are the eigenstates of the system *without* field) localized around  $k = 0$ . If the field is turned on, the  $k$ -states are no longer eigenstates and become time dependent. This time dependence causes the oscillatory motion. However, the wave packet can be expressed as well as a sum of Wannier–Stark states (the eigenstates *with* electric field) with certain weights. For the optical experiments, it is easier to conceive the photogenerated wave packet as a superposition of WS states. However, the mathematical expression of the Gedanken experiment wave packet and the photoexcited wave packet are directly connected by a unitary transition. The wave function and the dynamics of the wave packets can be made identical by a suitable choice of the wave packet parameters, as controlled by the spectrum of the optical excitation. The only difference between the Gedanken experiment and the optical experiments is the fact that optical experiments at the interband frequency are connected to the photoexcitation of holes, which influence the electronic properties of the system, as discussed below.

The equivalence of the transport Gedanken experiment and the optical experiments can also be demonstrated by another simple argument: the relevant parameters describing the oscillation dynamics of a wave packet are *the frequency and the spatial displacement*. As already pointed out, it is obvious that the transport Gedanken experiment and the optical experiment yield the same frequency. A discussion of the spatial extent of the oscillations is much more intricate, since the spatial amplitude depends critically on the initial composition of the wave packet.

Recently, the question of the spatial displacement has been investigated theoretically for Bloch oscillations in semiconductor SLs [27,28]. It turns out that the spatial extent of the Bloch wave packet oscillation is strongly dependent on the optical excitation conditions, but can reach, for certain parameters, the value given by (1.5), proving the equivalence of the experiments. In section 2.5, we discuss that the spatial displacement

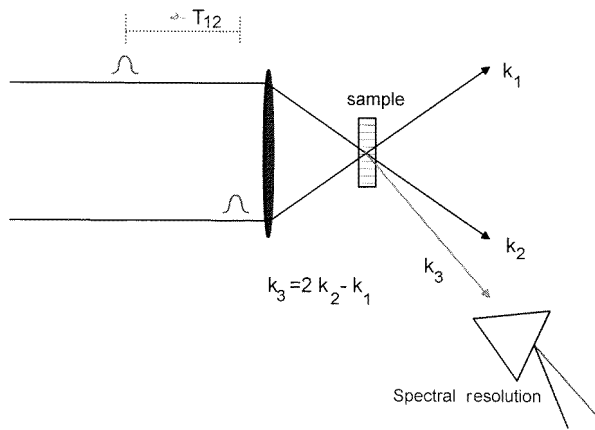


**Figure 4.** Scheme of the self-diffracted two-beam four-wave mixing experiment: the first pulse in direction  $k_1$  creates a polarization, the second pulse in direction  $k_2$  forms a grating. Part of pulse 2 is then diffracted in direction  $k_3$ . In the spectrally resolved variation of the experiment, the diffracted beam is analysed in a spectrometer.

can be measured experimentally and agrees well with the theoretical expectations.

The experimental observation of Bloch oscillations in superlattices has been reviewed a couple of years ago in an article [29] and in a later book [30]. A summary of the observation of the Wannier–Stark ladder, which briefly mentions Bloch oscillations, was given in [31].

## 2.2. Initial four-wave mixing experiments

The first experiments which observed BOs were performed using the two-beam transient four-wave mixing technique [32]. In this experiment (see figure 4), a first optical pulse with wave vector  $k_1$  creates the wave packet from a superposition of the WSL. A second, delayed pulse in direction  $k_2$  forms a grating with the (oscillating) polarization the first pulse has left over. Detected is the light diffracted from this grating into the a background-free direction  $k_3$ . In this direction, only a signal from coherent transitions is emitted. Bloch oscillations can be observed in a temporal observation of this signal, since the dipole moment between the electron wave packet and the hole will oscillate strongly due to the spatial motion. A detailed theoretical study of FWM in biased superlattices was given by von Plessen and Thomas [33]. Previously, Zakharov and Manykin had treated the FWM response of a bulk solid subject to an electric field [34].

The first experiment observing BOs by optical excitation of several transitions of the WSL was reported by Feldmann *et al* [14]. The experimental data showed a recovery of the FWM signal after a time period which was in agreement with the inverse WSL splitting. Later FWM experiments [15] showed clear oscillations of the FWM signal. For zero and low field, the FWM response shows quantum beats of the heavy-hole and light-hole excitons below the miniband. For somewhat higher fields, oscillations with a period which decreased linearly with bias voltage (i.e. field) were visible (figure 5). The FWM

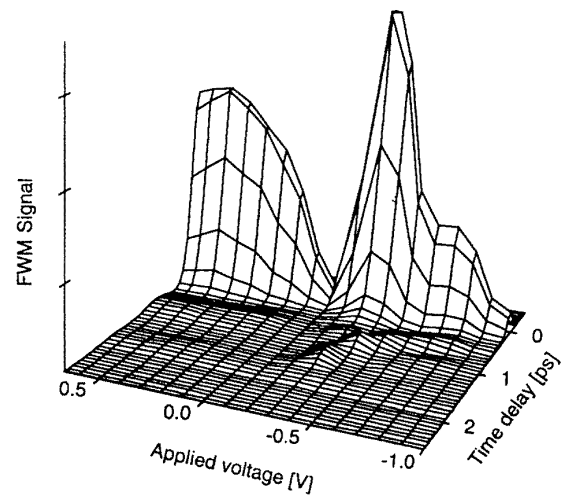


**Figure 5.** Three-dimensional plot of the low-temperature four-wave mixing signal as a function of the delay time and the voltage across the sample. Flat band is at +0.5 V. The sample is a 97 Å GaAs/17 Å  $\text{Al}_{0.3}\text{Ga}_{0.7}\text{As}$  superlattice. (From [36].)

scans for given fields showed oscillations with a period tunable over a large field range [15]: figure 6 shows scans of the FWM signal against delay for various electric fields. Figure 7 shows the splitting  $\Delta E$  as calculated from the experimentally measured period using (2.2) plotted against the electric field. The agreement of the oscillation periods with theory is good. Note that the tuning range extends from 2 to 10 meV splitting, i.e. over an oscillation frequency range of about 0.5 to 2.5 THz.

## 2.3. Detailed FWM experiments: quantum oscillations, miniband width dependence

A number of other studies using FWM with optical excitation have helped to improve the knowledge about BOs. One important experiment was the final demonstration that the observed effects were indeed due to quantum oscillations. It is a crucial point to show that the oscillatory signal observed by the FWM experiments are not caused by polarization interference effects: in simple FWM experiments, one cannot distinguish conclusively whether the oscillation seen is a true quantum-mechanical interference within a wave packet (as it is the case for BO) or whether it is caused by a far-field interference of the polarizations of different transitions of the WSL. Even in THz emission experiments (see below), one cannot exclude that the emission is due to the nonlinear mixing of two such polarizations.

A direct way to prove the quantum interference is spectrally resolved FWM: Tokizaki *et al* [35] have shown that spectral resolution of the diffracted beam can directly distinguish the two oscillation mechanisms. For quantum oscillations, the phase of the oscillations is not dependent on detection energy, for polarization oscillations, it is. Experiments by Leisching *et al* [36] have shown that the phase of the oscillations as observed in FWM is not dependent on the detection energy, thus

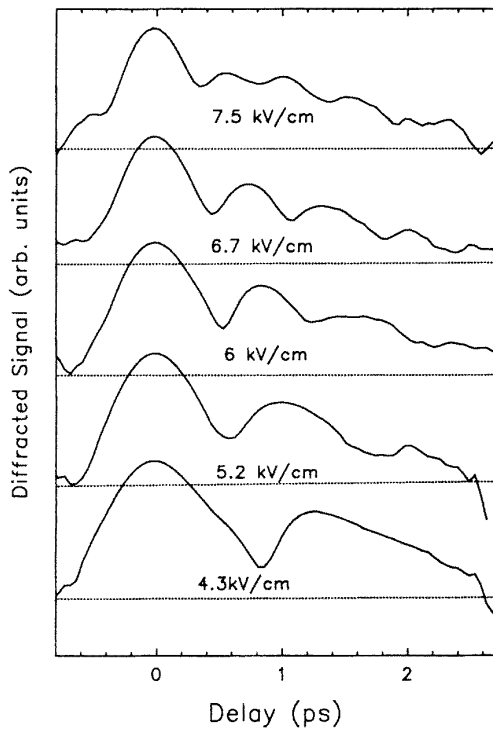


**Figure 6.** FWM scans for various electric fields. The sample is the same as described in the caption of figure 5.

proving unambiguously that the oscillations are quantum oscillations as expected for BOs. Figure 8 shows spectrally resolved FWM data for a  $67 \text{ \AA}$  GaAs/ $17 \text{ \AA}$   $\text{Al}_{0.3}\text{Ga}_{0.7}\text{As}$  sample. The phase of the oscillations is independent of detection energy, although the absolute FWM signal is changing strongly as a function of energy due to the strong spectral variation of the nonlinearity showing the WSL transitions. These data thus prove that the oscillations are caused by a quantum interference, as they should be if BOs are observed.

A more controversial topic has been the influence of miniband width on BOs. It was shown that BOs exist in GaAs/ $\text{Al}_{0.3}\text{Ga}_{0.7}\text{As}$  samples with miniband widths ranging from 19 to 50 meV [36]. There was no indication for a pronounced dependence of the BO damping on the miniband width. There is a lower limit in miniband width for optical studies of BOs: under a certain project miniband width, the Coulomb coupling prevents the formation of a miniband [20]. Nevertheless, field-tunable oscillations have been observed in this regime [37].

In the study of Leisching *et al* [36], a pronounced influence of the miniband width on the BOs was not observed, although the dephasing times were decreasing with increasing miniband width. Other researchers have claimed [38] from theoretical arguments that the optical phonon energy (which is of the order of 36 meV in GaAs SLs) would be a threshold where the damping as a function of the electric field would set in at lower field strengths. However, Bloch oscillations in samples with miniband width larger than the LO phonon energy have been observed [36], even at splittings  $eFd$  larger than reported in [38]. The question of the influence of miniband width on BOs is

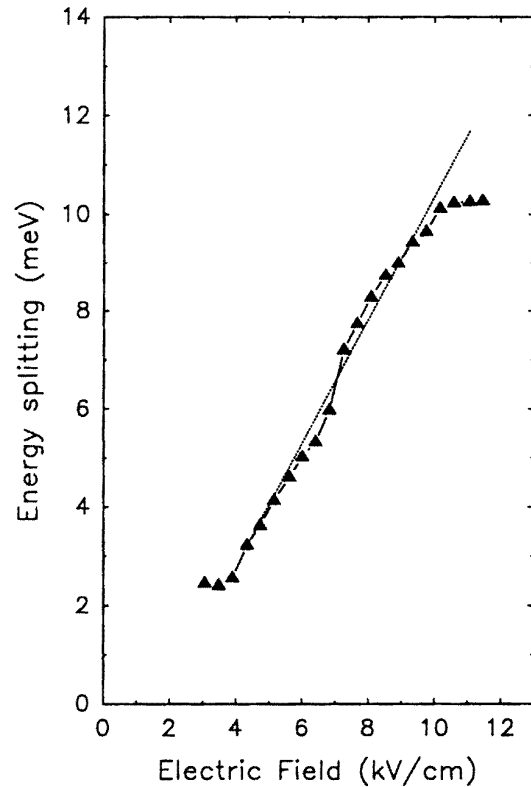


**Figure 7.** Splitting of the Wannier-Stark ladder, as obtained from the period of the Bloch oscillations in figure 6, against electric field. The dashed line is a guide for the eye.

closely related to the more general problem of the damping of BOs, which will be discussed in section 2.6.

#### 2.4. Experiments with intraband detection: THz spectroscopy

An impressive confirmation of the oscillation of the Bloch wave packets was the observation of THz emission of the wave packet by Waschke *et al* [16]. In this experiment, an optical pulse impinging onto the sample creates the Bloch wave packets. The oscillating dipole moment associated with the wave packet performing BOs causes radiation in the THz regime, which is detected with a small antenna which is gated with optical pulses producing a short in a fast photoconductor. Figure 9 shows data from [16]. These data confirm that the electrons performing Bloch oscillation emit THz radiation. As in the FWM experiments, this radiation can be tuned over a frequency range which is unusually large. In the experiments, the frequency was tuned between 0.5 and 2 THz. The upper limit, however, is given by the high-frequency cut-off of the antenna system. It can be expected that much higher frequencies for THz emission can be reached.

It is interesting to discuss the emitted power of the THz oscillator realized in the present experiment. A rough estimate of the emitted power, which depends strongly on the excitation condition assumed, yields values of the order of nano- to microwatts. The efficiency of the device is



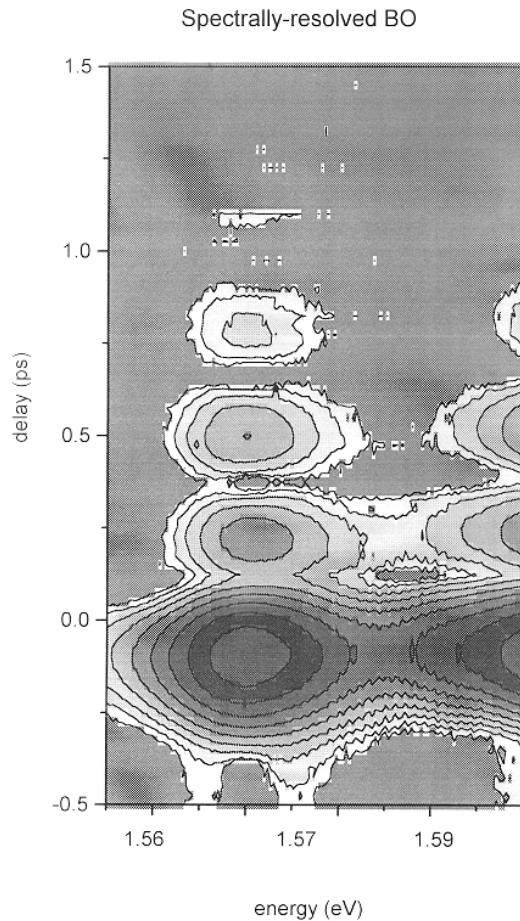


**Figure 8.** Contour plot of the spectrally resolved low-temperature FWM signal as a function of delay time and detection energy. The sample is a 67 Å GaAs/17 Å  $\text{Al}_{0.3}\text{Ga}_{0.7}\text{As}$  superlattice. It is clearly visible that the modulation due to the Bloch oscillations has the same phase for all energies, thus proving the quantum nature of the observation.

generally very low, mainly due to the fact that the interband energy put into the system by the optical excitation is lost when the hole and the electron move to the contacts. Thus, the efficiency of the device is already limited to values of the order of  $eFd/E_g$ , where  $E_g$  is the band gap of the well material. Typically, this ratio is of the order of  $10^{-3}$ . The second limitation for the optically excited THz emitter is the low density of carriers: the number of carriers which perform BOs is quite limited due to the fact that large numbers of optically excited carriers screen the static bias field and prevent the further observation of BOs [36]. Although the THz emission is a superradiant process and thus quadratic in density [39], it can be predicted that THz oscillators based on optical excitation will be constricted to very low emission powers.

It was initially believed that the THz signal directly reflects the intraband dynamics of the electrons and that the excitonic interaction does not influence the signals, in contrast to FWM experiments. Calculations in the framework of the semiconductor Bloch equations (SBEs) predicted that the dynamics after the decay of the interband

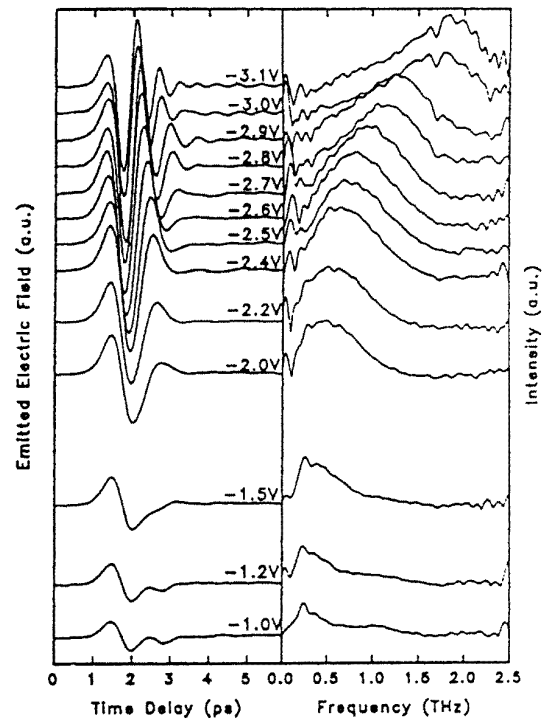


**Figure 9.** THz emission from a semiconductor superlattice. Shown is the measured THz field amplitude as a function of delay time for various electric fields. (From [16].)

polarization is not influenced by excitonic effects [40]. However, it was recently shown [41] that the SBEs are inadequate to describe the experiments. Newer theoretical approaches based on the dynamically controlled truncation (DCT) approach [42] predict that the THz signal is influenced by excitonic effects in a similar way to the FWM experiment. A recent comparison of THz and FWM results has confirmed this prediction [43]: it was shown that an anticrossing in the WSL (which is due to excitonic coupling) is mapped by both the THz and the FWM response.

## 2.5. Determination of the spatial displacement of Bloch oscillations

It has already been pointed out in the introduction that the identification of optical quantum beat experiments with Bloch oscillations in the sense of the transport Gedanken experiment sense depends crucially on the spatial amplitude of the oscillations. This amplitude can even be zero in the case of the *breathing mode* oscillation [25].

The spatial amplitude of optical experiments has been addressed in theoretical papers [27,28,44]. In the publication of Bouchard and Luban [28], the dynamics of the displacement were discussed in detail. However, the results were calculated in the single-particle picture, i.e. the excitonic coupling was neglected.

Dignam *et al* [27] have addressed the dynamics of wave packets including the excitonic interaction. In particular, they have calculated the displacement of the wave packet as a function of laser wavelength and band width. It turned

out that the amplitude can be continuously adjusted between zero (breathing mode) and the semiclassical limit given by (1.5). For symmetric excitation, i.e. when the laser spectrum is centred above the  $n = 0$  transition of the WSL, the amplitude is zero and the wave packet only performs a breathing mode motion. With increasing distance from the center of the WSL (both to lower and higher energy), the amplitude of the wave packet increases. When the centre of the laser spectrum is a few times the splitting of the WSL away from the centre, the amplitude for the semiclassical case as given in (1.5) is nearly reached.

The inclusion of the excitonic interaction leads to pronounced differences of the dependence on the laser parameters. In particular, an asymmetry for excitation below and above the centre of the WSL develops. The lower and upper limits for the amplitude are virtually unchanged, however: for excitation well (several times  $\Delta E$ ) above and below the centre of the WSL, the amplitude predicted by theory reaches about 95% of the semiclassical amplitude. It can thus be expected that optical experiments can come very close to the semiclassical amplitude.

There are several possible methods to determine the amplitude of BOs. The photorefractive sampling technique [17,45] seems to be a straightforward approach to determine the amplitude. However, a more detailed discussion has to take into account that the photorefractive coefficient at the excitonic band gap can be expected to be quite different from the bulk values. Thus, it is not possible to convert photorefractive data directly into amplitudes, without further calibration. The same reservation applies to an analysis of the THz data: a determination of the amplitude of the wave packet requires an *absolute* measurement of the THz emission, which is very difficult to achieve with the required precision. Also, the determination of the amplitude from the THz signal needs a theoretical calculation which links the THz intensity with the amplitude of the wave packet. Recent claims of amplitude measurements using THz emission have thus to be taken with a grain of salt [39]. Additionally, the data analysis of the authors of [39] depends critically on modeling the absorptive behaviour of metallic layers which were used as Schottky top contacts.

We have recently proposed [46,47] a new experiment which is capable of measuring the spatial displacement with high precision. The principal idea is very simple: as discussed above, the electrons perform spatial oscillations whereas the (heavy) holes stay virtually at the position where they are photoexcited. If the photoexcited electrons move to one side of the SL area, they create a negative charge at the front due to electrons and a positive charge at the back due to the holes left behind. Thus, the oscillating wave packets generate a small oscillating dipole field which is superimposed on the static bias field across the intrinsic region of the superlattice. This electric field is directly linked to the oscillation displacement  $z(t)$  by the relation

$$z(t) = \frac{en_{well}}{\epsilon_0\epsilon_r} \Delta E(t) \quad (2.3)$$

where  $n_{well}$  is the carrier density per well,  $\epsilon_r$  is the relative dielectric constant, and  $\Delta E$  is the energy shift

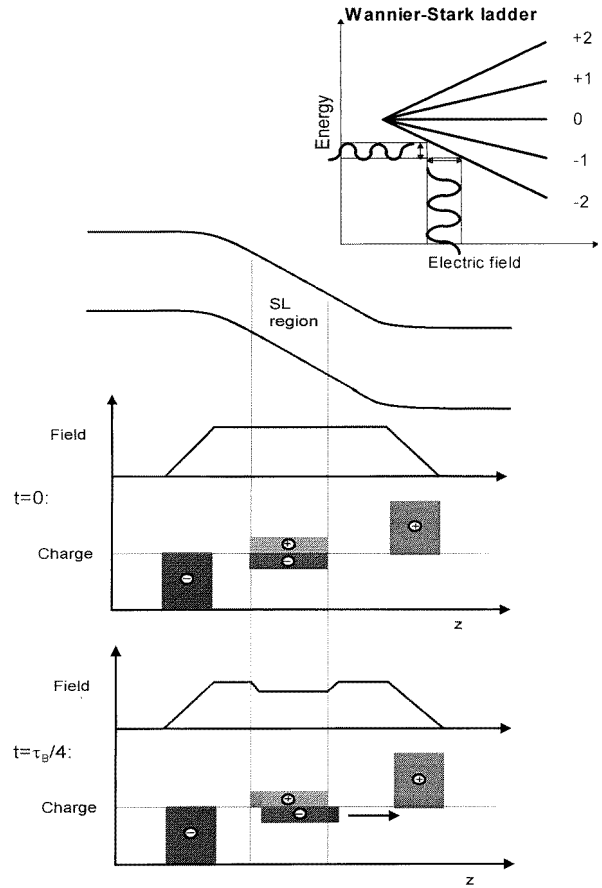


**Figure 10.** Schematic of the displacement experiment using the Wannier–Stark ladder as field sensor: when both electrons and holes are at the same place, the field is given by the static field created by the space charges of the pn-junction. If the electron wave packets move to the right, the field is reduced (bottom); for motion to the other side, the field would be enhanced. The oscillating field associated with the electron oscillation causes a motion up and down the WSL fan chart (upper right corner).

of a Wannier–Stark ladder transition with index  $n = 1$ . Transitions with higher  $n$  would show a correspondingly larger shift. This oscillating electric field can be detected using a very sensitive field sensor: the transitions of the WSL themselves.

Figure 10 displays a schematic picture of the experiment. Displayed are the field for zero displacement and for maximum displacement at a quarter of  $\tau_B$ . In the region of the sample where the BOs take place, the static field is lowered (or increased for a motion into the other direction) due to additional small space charges. The inset at the top right of the figure shows the field moving up and down the WSL fan chart which goes along with the BOs.

The shift of the WSL transitions can in principle be detected by various techniques, e.g. time-resolved transmission or FWM experiments. Figure 11 shows several electron to heavy hole (hh) transitions of a WSL ladder as observed by FWM as a function of delay time. The various spectra shown correspond to delay times of the first part (solid lines) and the second part (dashed lines) of one cycle of the BOs. Shown are the centre transition of

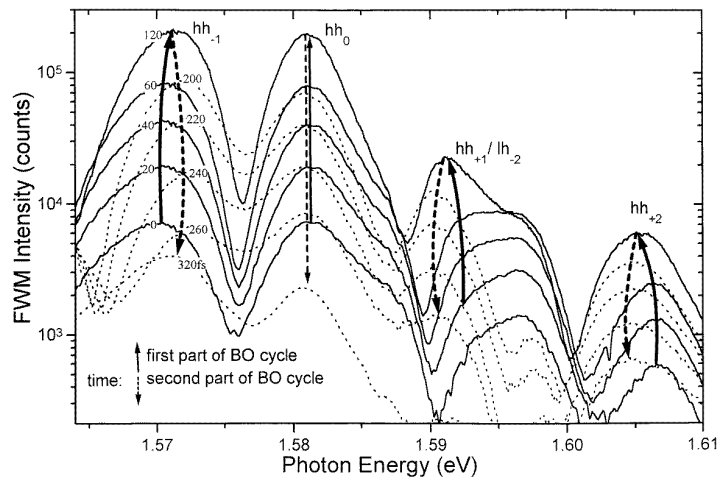


**Figure 11.** Shift of different transitions of the Wannier–Stark ladder for various delay times during one oscillation cycle. Solid arrows mark the behaviour during the first part of the cycle, dashed arrows during the second.

the WSL ( $hh_0$ ), the first transition below the centre ( $hh_{-1}$ ), and two transitions above the centre. The  $hh_{-1}$  transition shows a shift to lower energy of the order of a fraction of an meV during the first part of the BO cycle. During the second part, it shifts back to its original position. The  $hh_0$  centre transition stays at virtually constant energy, whereas the  $hh_{+2}$  transition shifts first to higher energy and then to lower energies, with an amplitude which is larger than for the  $hh_{-1}$  transition. The transitions thus clearly follow the behaviour as expected from the discussion above (see also figure 10).

The  $hh_{+1}$  transition shows a much more complicated behaviour than the other transitions. This is caused by the fact that it is subject to an anticrossing with a higher transition in the static field region which is shown in figure 11. The fact that the transition displays this anticrossing even in the dynamic field situation is a further proof that the field shifts of the WSL directly trace the dynamics of the oscillation. We have recently shown that tracing such an anticrossing reveals the displacement dynamics as well [48].

The shift of the  $hh_{-1}$  WSL transition is displayed in figure 12. For this figure, a rather high excitation density was chosen to make the effect of the field shifts clearer. The peak positions plotted in the figure have been obtained by a fit of a Gaussian line shape to the spectra. The data show a sinusoidal shift of the peak with delay time. It is clearly visible from figure 12 that the field shift of the WSL peak decreases with increasing delay time. This decay of the field shift is not due to a decay of the wave packet amplitude, but due to a decrease of the number of carriers which coherently participate in the BO: carriers which have lost the coherence do not contribute to the oscillating electric field any longer. A comparison of the dephasing time of the FWM signal with the decrease of the field shift amplitude shows good agreement, in support of this explanation. The solid line is a harmonic function assuming a dephasing time of 1.2 ps, in good agreement with independent measurements (see below, section 2.6).

The displacement of the BO wave packet can be easily obtained by the relation between field shift and oscillation

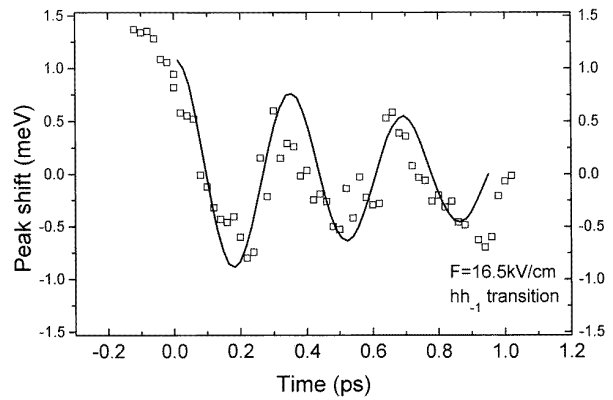


**Figure 12.** Wannier–Stark ladder peak shift as a function of delay time for a  $67 \text{ \AA}/17 \text{ \AA}$  superlattice. The solid line is a damped harmonic with a damping time of 1.2 ps.

displacement given by (2.3). A correction for the decay of the number of coherent carriers has to be made by dividing the field shift by an exponential with the decay time. The result is plotted as the left (displacement) axis in figure 13. The wave packet performs an oscillation with a total amplitude of approximately  $160 \text{ \AA}$ . Within error, the displacement as a function of time follows a harmonic function. This is expected for a miniband with harmonic dispersion. A numerical calculation of the miniband dispersion in our samples using the transfer-matrix approximation shows that the miniband in these deep wells is very close to the harmonic case. It is interesting to note that the direct measurement of the displacement of BO is thus also a method to directly measure the dispersion of minibands in superlattices.

The field detection by shifts of the WSL can also trace the dynamics of the *incoherent* carriers: the electrons and holes which have lost the coherence and are moved by drift transport to the contacts lead to a small linear shift which is superimposed on the harmonic shift of the WSL transitions. It can be assumed that this transport of carriers is a sequence of drift transport and Bloch oscillations. An

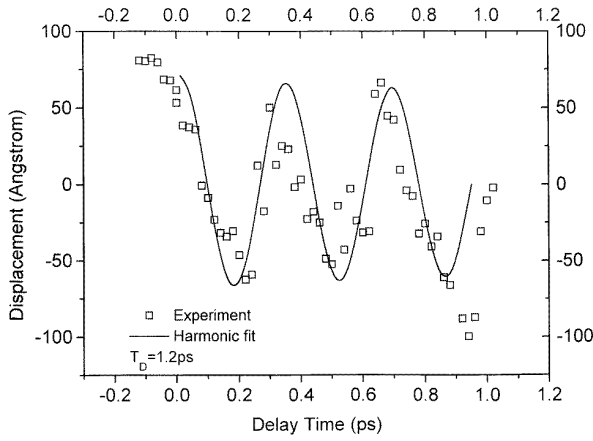


**Figure 13.** Bloch electron displacement as a function of delay time for a 67 Å/17 Å superlattice.

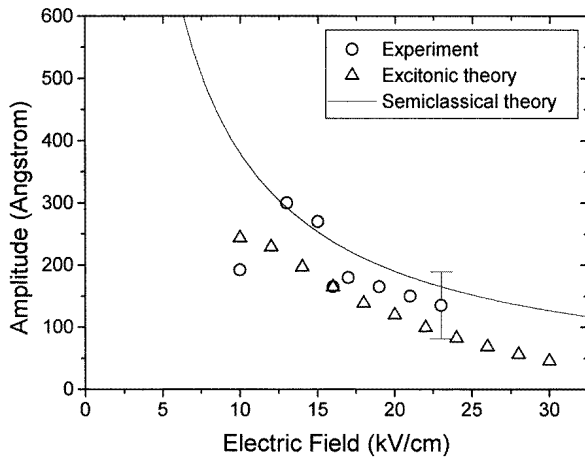


**Figure 14.** Total oscillation amplitude as a function of the electric field. Circles: experiment, line: semiclassical theory, triangles: theory including optical excitation of the wave packet and excitonic interactions.

analysis of this regime should be possible by a study of the linear shift as a function of parameters like the field and temperature.

The dependence of the Bloch oscillation amplitude on the electric field is shown in figure 14. The experimental data are the circles. The solid line is the semiclassical limit which is given by (1.5). It is obvious that the experimental data are, within error, in reasonable agreement with the semiclassical theory. The amplitude is inversely decreasing with electric field as predicted. For lower field values, the experimental data start to deviate from the semiclassical theory. A more detailed analysis of this field region shows that the anticrossings between the various states (e.g. the miniband excitons crossing the WSL states) lead to a complicated dependence of the wave packet amplitude on the excitation conditions [49].

The influence of excitonic effects on the amplitude of the Bloch wave packet has been theoretically analysed in detail [27]. It was shown that the upper limit of the amplitude as given by the semiclassical theory (1.5) remains virtually unchanged. However, the amplitude depends on

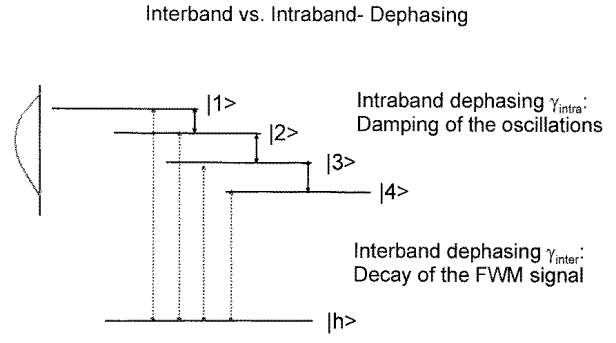


**Figure 15.** Scheme of interband (dashed arrows) and intraband (solid arrows) dephasing in a superlattice between the electron ladder and the hole state.

the detailed excitation conditions. The triangles in figure 14 show a calculation for our excitation parameters following the excitonic model described in [27]. The amplitudes are somewhat lower than the semiclassical limit and in good agreement with the experimental data. The main reason for the lower amplitudes predicted by the excitonic theory (in comparison to the semiclassical results) is not the electron–hole coupling, but the fact that our excitation was rather close to the centre of the WSL.

## 2.6. Damping of Bloch oscillations

One problem which is still not sufficiently clarified is the question of the damping mechanisms of BOs. This question is important both for applications and for the basic understanding of the physics of wave packet dynamics in superlattices. One has to distinguish the different dephasing mechanisms which apply when optically excited wave packet experiments are discussed: figure 15 shows a schematical picture of the situation for optical experiments studying dephasing. The BOs are damped if the phase relation between the constituents of the wave packet is lost. The critical parameter for this is the *intraband* damping rate  $\gamma_{intra} = 1/T_2^{intra}$ , where  $T_2^{intra}$  is the dephasing time. The intraband damping can be caused by transitions between states of the WSL, transitions to higher bands and by coupling of the WSL to a bath. The intraband damping has to be distinguished from the interband damping time  $\gamma_{inter} = 1/T_2^{inter}$ , which is related to the dephasing between the photoexcited electron and hole. It has been shown that these dephasing times can be quite different and that the intraband dephasing time in superlattices is longer than the interband time [50].

In the FWM signals, the decay of the *envelope of the overall FWM signal* is related to the interband dephasing. The decay of the envelope is given by  $T_2^{inter}/2$  if the transition is homogeneously broadened and  $T_2^{inter}/4$  if it is inhomogeneously broadened. However, the damping of the modulation of the FWM signal is not caused by the interband dephasing, but by intraband dephasing. The simplest model to discuss the dephasing channels is to treat the system—hole states/electron WSL states—as a three-level system. The dephasing of three-level systems has been analysed in [12]. If one assumes that the difference

between the interband dephasing of the two upper states is only due to intraband scattering between the two states, the damping of the BO which modulates the FWM decay is given by the intraband dephasing only. This damping time can be obtained by a fit to the FWM decay with an exponential which is modulated with a damped harmonic function. Using such an analysis, a systematic study of BO damping was recently performed [51, 52]. The results have shown that the intraband damping time as derived from the damping of the harmonic modulation is typically much longer than the interband damping time as derived from the overall decay time of the FWM signal. The results showed that the dephasing at higher temperatures is due to scattering by optical phonons. At low temperatures, however, the damping is dominated by a term which is both temperature and density independent, i.e. neither caused by carrier-carrier scattering nor phonon scattering. The damping as a function of density showed in the investigated range ( $1 \times 10^8 \text{ cm}^{-2}$  to  $1.5 \times 10^9 \text{ cm}^{-2}$ ) no dependence of the intraband damping rate on density. Recent studies using the detection of THz emission [39] to study the intraband damping showed a linear increase of  $\gamma_{intra}$  in the density range of  $2 \times 10^9 \text{ cm}^{-2}$  to  $2 \times 10^{10} \text{ cm}^{-2}$ . The absolute value of the damping rate between the FWM measurements [51] mentioned above and the THz results agrees quite well. One can thus conclude that the damping of the optically generated wave packets is governed by a density-independent term at low density and a linearly increasing term at higher densities. The latter term is expected for exciton-exciton scattering and has, for example, been observed in the interband dephasing rate of quantum wells as a function of exciton density [53].

Possible mechanisms which can explain the density-independent term at low densities are (i) scattering at the interfaces of the superlattice or (ii) a completely different physical mechanism: the superposition of several states of the WSL which are not equidistant (due to the Coulomb interaction) will lead to a destructive interference. It was shown in [51] and [52] that the BOs disappear completely if many transitions of the WSL are excited simultaneously. Figure 16 shows spectrally resolved FWM signals against delay time for excitation of a large number of WSL states. The different traces refer to the different detection energies. They are labelled with the transition indices which are displayed in the inset, together with the spectrum of the laser pulse used for excitation. It is obvious that the oscillations are nearly completely suppressed for most of the detection energies. This effect can be explained by the interference of many non-equidistant levels of the WSL. However, one has to note that this experiment cannot completely exclude other effects for the fast dephasing: when many levels of the WSL are excited, it cannot be avoided that a considerable number of free carriers are excited in the continuum of the WSL states with lower index.

The damping properties were recently investigated theoretically by two groups [54, 55]. It was pointed out that the damping of the THz radiation due to carrier-carrier scattering is caused by the electron intraband damping [54] and is expected to be much longer than the interband

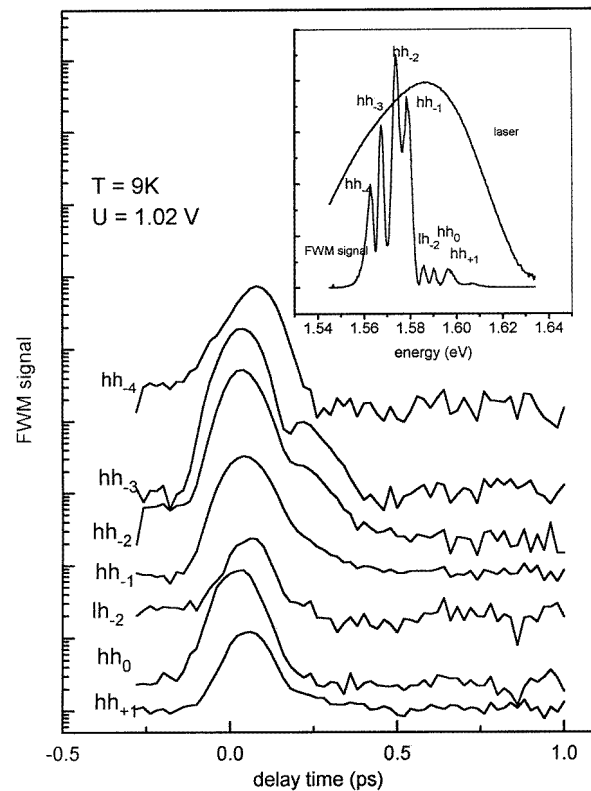


**Figure 16.** Spectrally resolved FWM signal for various transitions of the WSL for excitation of a large number of transitions. The transition labels give the Wannier-Stark ladder peak where the detection energy has been chosen. The inset shows the laser spectrum together with the WSL. Note that the Bloch oscillations are nearly washed out due to the interference of a large number of transitions.

damping, as experimentally observed [51]. In [55], the influence of interface roughness on the damping dynamics of Bloch oscillations was investigated. It was shown that the interface roughness leads to scattering which can be described by a single, field-independent scattering time. Bloch oscillations are observed if the static field is large enough that the Bloch period is shorter than this time.

A remarkable result which is related to the damping of BOs is the observation by Roskos *et al* [56] that BOs can be observed even if the interband optical excitation is creating carriers in the second miniband. Since the relaxation by LO phonons is much faster than the BO periods, it can be concluded that the carriers relax to the first miniband and then perform the BOs. The scattering down to the first miniband seems to preserve the intraband coherence. The interband coherence is obviously lost in this process, as is known from the very fast disappearance of the FWM signal once the excitation is tuned away from the band edge.

### 3. Comparison to transport and further experiments

#### 3.1. Electrical transport experiments

Electrical transport experiments have brought a detailed understanding of carrier motion in narrow bands. The first

experiments in superlattices were reported soon after the proposal of the structures [8]. Clear evidence for effects due to field localization were reported in a series of papers by Sibille and coworkers [57–59]. Besides the observation of negative differential conductivity (NDC), a particularly illuminating experiment was the direct proof [60] that the NDC starts to occur in the same field range where the WSL is observed in the optical response. This experiment directly relates the transport and optical picture of the BOs and WSL effects. It is also a proof that there is no low-field range where BO can take place *without* the presence of the WSL. As mentioned above, the standard transport experiments do not give direct evidence for BOs since one measures properties which are averaged over an ensemble of carriers without defined phase relations.

### 3.2. Combination of transport experiments with THz radiation

The absorption and emission of semiconductor superlattices with and without electrical bias have been studied in detail. A comprehensive review has recently been given in this journal by Helm [61]. A number of experiments have been performed in the regime where the bias fields are zero or low enough that the miniband is preserved (i.e. the field localization length is larger than the coherence length). The absorption experiments have shown both the characteristic features of inter- [62] and intra-miniband [63] absorption. Absorption between the states of the WSL has not been reported yet. Actually, it was theoretically predicted [65] that the absorption disappears. Up to now, no reports for electrically generated intra-miniband emission have been reported.

Emission studies from biased superlattices have recently brought exciting results. The first experiment which has shown spontaneous emission due to intraband emission was reported by Helm *et al* [64]. The intensity of this radiation was quite low. Far-infrared experiments which address the intra-miniband properties when the WSL is present have not been performed.

A field which has been recently investigated in detail is the influence of THz radiation (in the far-infrared (FIR)) on the transport in superlattices. It was shown that the  $I$ – $V$  curve of the superlattice is strongly changed when FIR is focused onto the sample [66,67]. The observed effects were explained by a theoretical model based on nonlinear transport in superlattices [68]. The main parameter which can be deduced from the observed effects is the scattering time of the electrons. This time is in principle identical to what is measured as intraband dephasing in the optical experiments. It is an interesting future task to check the similarities and differences in the damping behaviour of the far-infrared and interband optical experiments.

Recently, the *inverse Bloch oscillator* was observed [69]. In this experiment, the current through the superlattice showed resonances when the frequency of the radiation was tuned through multiples of the BO frequency.

### 3.3. Further experiments in semiconductors

Although the research on Bloch oscillations has made considerable progress in the last few years, there are a number of problems which need to be challenged. In the following, two of them will be briefly discussed.

**3.3.1. How close can we come to the Bloch oscillation Gedanken experiment?** The first step from the interband optical experiment to the true transport Gedanken experiment would be to perform an experiment where the BOs are restricted to electrons only and the Coulomb coupling to holes can be avoided. One approach is to still use the elegant and efficient way of generating the coherent electron wave packets with laser pulses, but restrict the oscillation to a region where only electrons are present. However, up to now, no experimental scheme to accomplish the injection of the photo-generated electrons into a region without holes has been proposed.

The next step would be the realization of Bloch oscillations completely without optical excitation. The challenge is to create Bloch electron wave packets with well defined relative phase. One approach to reach a defined phase relation is the Gedanken experiment method of switching the field in a time period which is short compared to  $\tau_B$ . This is difficult since the switching times required in semiconductor superlattices are less than 1 ps. Electric pulses of such a duration can be created using optical techniques. It is possible to let such pulses propagate along strip lines. However, it is difficult to conceive an arrangement where a step-function electric field across a pin-structure is applied on such a time scale.

A second, more prospective approach to achieve defined phase relations is to implement some feed-back mechanisms. Such an approach has been proposed for the related system of coupled double quantum wells by Luryi [70]. He has shown that a system with feedback can oscillate when it is excited with a cw laser. The relevant question for the experimental realization is the design of the feedback loop. One approach would be to couple back the THz radiation by a suitable mirror structure. However, serious proposals for a structure have not yet been made.

**3.3.2. Realization of electrically driven emitters: the Bloch oscillator.** It is very likely that devices which emit THz radiation will only be used for broad applications if they directly convert electric power into the emitted radiation. Thus, structures which need pulsed optical excitation for operation are unlikely to yield useful devices. Furthermore, the efficiency and absolute power levels attainable by such devices seem to be rather low, as discussed above.

Recently, semiconductor heterostructures have been used to realize lasers which involve only transitions in the conduction band of semiconductors. Initial structures [71] used laser transitions between coupled quantum wells. More recently, a superlattice laser has been realized [72]. This laser uses the interband transition between the lower edge of the second miniband and the upper edge of the first miniband, both located at the edge of the mini-Brillouin

zone. This scheme has the advantage of easily achieving inversion due to the fact that the intraband relaxation time (which populates the upper laser level and depopulates the lower laser level) is fast compared to the interminiband relaxation time. The devices reported so far have very high power. The wavelengths of the device seem to be easily scalable from the presently achieved  $\lambda = 11 \mu\text{m}$  to the farther infrared. It is then clear that any Bloch oscillator device has to compete with these very efficient intraband lasers. The only key advantage a Bloch oscillator or laser could have over those structures is a large *in situ* tunability. It remains to be seen whether a practical device will be realized.

#### 4. Conclusions

In this review, I have discussed the recent interband optical experiments investigating Bloch oscillations in semiconductor superlattices. The experiments have unambiguously shown that the photo-excited electron wave packets perform spatial oscillations which follow the predictions made by Bloch and Zener in the 1930s. Together with the intraband optical studies and transport experiments performed in superlattices, the results give a consistent, albeit not complete, picture of the physics of Bloch oscillations. Further experimental work has to clarify mostly the relaxation phenomena, which are still little understood.

Furthermore, it will be interesting to see whether the concept of Bloch oscillations will lead to useful devices. Up to now, not much more than the fact that the oscillations are leading to an emission of THz radiation has been achieved. Potentially, Bloch oscillations could be used to realize coherent far-infrared sources with an extremely large tunability.

#### Acknowledgments

It is a pleasure for me to acknowledge the many persons I collaborated with in the investigation of Bloch oscillations. First, I would like to thank the persons who made the key experiments possible: Jochen Feldmann, Peter Haring Bolivar, Klaus Köhler, Patrick Leisching, Vadim Lyssenko, Hartmut Roskos and Jagdeep Shah. Invaluable have also been contributions from Wolfgang Beck, Marc Dignam, Peter Ganser, Tom Hasche, Falk Löser, Markas Sudzius, Gintaras Valusis and Christian Waschke. Also, I would like to acknowledge the many persons who have contributed by discussions: Huib Bakker, Daniel Chemla, David Dunlap, Daniel Loss, David Miller, Gero von Plessen, Karl Renk, Karl Unterrainer and Heinrich Kurz, who has also provided excellent experimental facilities for the experiments performed at Aachen. Large parts of the work reported here would not have been possible without support from the Deutsche Forschungsgemeinschaft (contracts Le 747/2-1, 10-1, 11-1, 11-2 and through the Graduiertenkolleg 'Struktur- und Korrelationseffekte in Festkörpersystemen'), the Land Nordrhein-Westfalen through the 'Bennigsen-Foerder-Preis', and the Alfried-Krupp Stiftung.

#### References

- [1] Drude P 1900 *Ann. Phys., Lpz* **1** 566  
Drude P 1900 *Ann. Phys., Lpz* **3** 369  
For a lucid discussion of Drude transport, see [4] ch 1
- [2] Bloch F 1928 *Z. Phys.* **52** 555
- [3] Zener C 1934 *Proc. R. Soc. A* **145** 523
- [4] See, e.g. Ashcroft N W and Mermin N D 1981 *Solid State Physics* Int. edn (Tokyo: Holt-Saunders) p 225
- [5] It is interesting to note that scattering processes are necessary to have transport occurring in a single band: if no scattering processes were present, the carriers would perform periodic oscillations in space and time, but would stay on average at the same spatial position.
- [6] Wannier G H 1969 *Phys. Rev.* **117** 432. The first prediction for the ladder-like structure was actually given by James H M 1949 *Phys. Rev.* **76** 1611
- [7] Esaki L and Tsu R 1970 *IBM J. Res. Dev.* **61** 61
- [8] Esaki L, Chang L L, Howard W E and Rideout V L 1972 *Proc. 11th Conf. on Physics of Semiconductors (Warsaw, 1972)* (Warsaw: Polish Scientific Publishers) p 431
- [9] Esaki L and Chang L L 1974 *Phys. Rev. Lett.* **33** 495
- [10] Dingle R, Gossard A C and Wiegmann W 1975 *Phys. Rev. Lett.* **34** 1327
- [11] Tsu R, Chang L L, Sai-Halasz G A and Esaki L 1975 *Phys. Rev. Lett.* **34** 1509
- [12] Leo K, Shah J, Göbel E O, Damen T C, Schmitt-Rink S, Schäfer W and Köhler K 1991 *Phys. Rev. Lett.* **66** 201
- [13] Roskos H G, Nuss M C, Shah J, Leo K, Miller D A B, Fox A M, Schmitt-Rink S and Köhler K 1992 *Phys. Rev. Lett.* **68** 2216
- [14] Feldmann J, Leo K, Shah J, Miller D A B, Cunningham J E, Schmitt-Rink S, Meier T, von Plessen G, Schulze A and Thomas P 1992 *Phys. Rev. B* **46** 7252
- [15] Leo K, Haring Bolivar P, Brüggemann F, Schwedler R and Köhler K 1992 *Solid State Commun.* **84** 943
- [16] Waschke C, Roskos H G, Schwedler R, Leo K, Kurz H and Köhler K 1993 *Phys. Rev. Lett.* **70** 3319
- [17] Dekorsy T, Leisching P, Köhler K and Kurz H 1994 *Phys. Rev. B* **50** 8106
- [18] Cho G C, Dekorsy T, Bakker H J, Kurz H, Kohl A and Opitez B 1996 *Phys. Rev. B* **54** 4420
- [19] Bastard G 1988 *Wave Mechanics Applied to Semiconductor Heterostructure* (Les Ulis: Les Editions de Physique) p 63
- [20] Fox A M, Miller D A B, Cunningham J E, Jan W Y, Chao C Y P and Chuang S L 1992 *Phys. Rev. B* **46** 15365
- [21] Ben Dahan M, Peik E, Reichel J, Castin Y and Salomon C 1996 *Phys. Rev. Lett.* **76** 4508
- [22] Sibille A, Palmier J F, Wang H and Mollot F 1990 *Phys. Rev. Lett.* **64** 52
- [23] Mendez E E, Agullo-Rueda F and Hong J M 1988 *Phys. Rev. Lett.* **60** 2426
- [24] Voisin P, Bleuse J, Bouche C, Gaillard S, Alibert C and Regreny A 1988 *Phys. Rev. Lett.* **61** 1639
- [25] Bastard G and Ferreira R 1989 *Spectroscopy of Semiconductor Microstructures (NATO Advance Study Institute, Series B: Physics 206)* ed G Fasol and A Fasolino (New York: Plenum) p 333
- [26] 1994 Dunlap D private communication
- [27] Dignam M, Sipe J E and Shah J 1994 *Phys. Rev. B* **49** 10502
- [28] Bouchard A M and Luban M 1993 *Phys. Rev. B* **47** 6815
- [29] Feldmann J 1992 *Festkörperprobleme/Adv. Solid State Phys.* **32** 81
- [30] Agullo-Rueda F and Feldmann J 1995 *Semiconductor Superlattices—Growth and Electronic Properties* ed H T Grahn (Singapore: World Scientific)

- [31] Mendez E E and Bastard G 1993 *Phys. Today* **34** 35
- [32] Yajima T and Taira Y 1979 *J. Phys. Soc. Japan* **47** 1620
- [33] von Plessen G and Thomas P 1992 *Phys. Rev. B* **45** 9185
- [34] Zakharov S M and Manykin E A 1973 *Izv. Akad. Nauk SSSR* **37** 2171
- [35] Tokizaki T, Nakamura A, Ishida Y, Yahima T, Akai I and Karasawa T 1990 *Ultrafast Phenomena VII (Springer Series in Chemical Physics 53)* ed C B Harris, E P Ippen, Mourou G A and Zewail A H (Berlin: Springer) p 253
- [36] Leisching P, Haring Bolivar P, Beck W, Dhaibi Y, Brüggemann F, Schwedler R, Kurz H, Leo K and Köhler K 1994 *Phys. Rev. B* **50** 14 389
- [37] Cohen G, Bar-Joseph I and Shtrikman H 1994 *Phys. Rev. B* **50** 17 316
- [38] von Plessen G, Meier T, Feldmann J, Göbel E O, Thomas P, Goossen K W, Kuo J M and Kopf R F 1994 *Phys. Rev. B* **49** 14 058
- [39] Martini R, Klose G, Roskos H G, Kurz H, Grahn H T and Hey R 1996 *Phys. Rev. B* **54** R14 325
- [40] Meier T, Rossi F, Thomas P and Koch S W 1995 *Phys. Rev. Lett.* **75** 2558
- [41] Axt V M, Bartels G and Stahl A 1996 *Phys. Rev. Lett.* **76** 2543
- [42] Axt V M and Stahl A 1994 *Z. Phys. B* **93** 195
- [43] Haring Bolivar P, Wolter F, Müller A, Roskos H G, Kurz H and Köhler K 1997 *Phys. Rev. Lett.* **78** 2232
- [44] Biermann M L and Stroud C R Jr 1993 *Phys. Rev. B* **47** 3718
- [45] Ralph S E, Capasso F and Malik R J 1989 *Phys. Rev. Lett.* **63** 2272
- [46] Lyssenko V G, Valusis G, Löser F, Hasche T, Leo K, Dignam M M and Köhler K 1997 *Phys. Rev. Lett.* **79** 301
- [47] Lyssenko V G, Valusis G, Löser F, Hasche T, Leo K, Köhler K and Dignam M M 1996 *Proc. 23th Int. Conf. on Physics of Semiconductors (Berlin, 1996)* ed M Scheffler and R Zimmermann (Singapore: World Scientific) p 1763
- [48] Sudzius M, Löser F, Lyssenko V G, Leo K, Oignam M M and Köhler K 1998 unpublished
- [49] Lyssenko V G, Sudzius M, Löser F, Valusis G, Hasche T, Leo K, Dignam M M and Köhler K 1998 *Festkörperprobleme/Adv. Solid State Phys.* to be published
- [50] Leisching P, Dekorsy T, Bakker H J, Kurz H and Köhler K 1995 *Phys. Rev. B* **51** 18 015
- [51] Valusis G, Lyssenko V G, Klatt D, Pantke K-H, Löser F, Leo K and Köhler K 1996 *Proc. 23th Int. Conf. on Physics of Semiconductors (Berlin, 1996)* ed M Scheffler and R Zimmermann (Singapore: World Scientific) p 1783
- [52] Valusis G 1997 personal communication
- [53] Schultheis L, Honold A, Kuhl J and Tu C W 1986 *Phys. Rev. B* **34** 9027
- [54] Rossi F, Gulia M, Selbmann P E, Molinari E, Meier T, Thomas P and Koch S W 1996 *Proc. 23th Int. Conf. on Physics of Semiconductors (Berlin, 1996)* ed M Scheffler and R Zimmermann (Singapore: World Scientific) p 1775
- [55] Diez E, Dominguez-Adame F and Sanchez A unpublished
- [56] Roskos H G, Waschke C, Schwedler R, Leisching P, Dhaibi Y, Kurz H and Köhler K 1994 *Superlatt. Microstruct.* **15** 281
- [57] Sibille A, Palmier J F, Wang H and Mollot F 1990 *Phys. Rev. Lett.* **64** 52
- [58] Sibille A, Palmier J F, Hadjazi M, Wang H, Etemadi G and Dutisseuil E 1993 *Superlatt. Microstruct.* **13** 247
- [59] Lee M, Solin S A and Hines D R 1993 *Phys. Rev. B* **48** 11 921
- [60] Sibille A, Palmier J F and Mollot F 1992 *Appl. Phys. Lett.* **60** 457
- Palmier J F and Mollot F 1994 *Ann. Phys., Lpz* **3** 137
- [61] Helm M 1995 *Semicond. Sci. Technol.* **10** 567
- [62] Helm M, Hilber W, Fromherz T, Peeters F M, Alavi K and Pathak R N 1993 *Phys. Rev. B* **48** 1601
- [63] Brozak G, Helm M, DeRosa F, Perry C H, Koza M, Bhat R and Allen S J 1990 *Phys. Rev. Lett.* **64** 3163
- [64] Helm M, England P, Colas E, DeRosa F and Allen S J 1989 *Phys. Rev. Lett.* **63** 74
- [65] Bastard G and Ferreira R 1991 *C. R. Acad. Sci. Paris* **312** II 971
- [66] Ignatov A A, Schomburg E, Renk K F, Schatz W, Palmier J F and Mollot F 1994 *Ann. Phys., Lpz* **3** 137
- [67] Schomburg E, Ignatov A A, Grenzer J, Renk K F, Pavel'ev D G, Koschurinov Yu, Melzer B Ja, Ivanov S, Schaposchnikov S and Kop'ev P S 1996 *Appl. Phys. Lett.* **68** 1096
- [68] Ignatov A A, Renk K F and Dodin E P 1993 *Phys. Rev. Lett.* **70** 1996
- [69] Unterrainer K, Keay B J, Wanke M C, Allen S J, Leonard D, Medeiros-Ribeiro G, Bhattacharya U and Rodwell M J 1996 *Phys. Rev. Lett.* **76** 2973
- [70] Luryi S 1991 *IEEE J. Quantum Electron.* **27** 54
- [71] Faist J, Capasso F, Sivco D L, Sirtori C, Hutchison A L and Cho A Y 1994 *Science* **264** 553
- [72] Scamarcio G, Capasso F, Sirtori C, Faist J, Hutchison A L, Sivco D L and Cho A Y 1997 *Science* **276** 773